analytical chemistry

pubs.acs.org/ac Article

A CRISPR/Cas12a-Mediated Dual-Mode Electrochemical Biosensor for Polymerase Chain Reaction-Free Detection of Genetically Modified Soybean

Haoran Ge, Xiaofu Wang,* Junfeng Xu, Han Lin, Huiqian Zhou, Tingting Hao, Yangbo Wu, and Zhiyong Guo*

Cite This: *Anal. Chem.* 2021, 93, 14885−14891 Read Online

ACCESS | Metrics & More | Article Recommendations | Supporting Information

ABSTRACT: A clustered regularly interspaced short palindromic repeats (CRISPR)/Cas12a-mediated dual-mode electrochemical biosensor without polymerase chain reaction (PCR) amplification was designed for sensitive and reliable detection of genetically modified soybean SHZD32-1. A functionalized composite bionanomaterial Fe_3O_4@AuNPs/DNA-Fc&Ru was synthesized as the signal unit, while a characteristic gene fragment of SHZD32-1 was chosen as the target DNA (tDNA). When Cas12a, crRNA, and tDNA were present simultaneously, a ternary complex Cas12a-crRNA-tDNA was formed, and the nonspecific cleavage ability of the CRISPR/Cas12a system toward single-stranded DNA was activated. Thus, the single-stranded DNA-Fc in the signal unit was cleaved, resulting in the decrease in the fast scan voltammetric (FSV) signal from ferrocene (Fc) and the increase in the electrochemiluminescence (ECL) signal from ruthenium complex (Ru) inhibited by Fc. The linear range was $1-10^7$ fmol/L for ECL and $10-10^8$ fmol/L for FSV, and the limit of detection (LOD) was 0.3 fmol/L for ECL and 3 fmol/L for FSV. Accuracy, precision, stability, selectivity, and reliability were all satisfied. In addition, PCR-free detection could be completed in an hour at room temperature without requiring complicated operation and sample processing, showing great potential in the field detection of genetically modified crops.

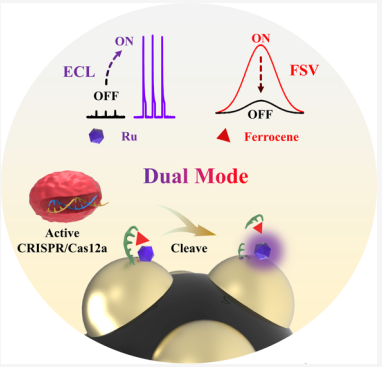

INTRODUCTION

Genetically modified organisms (GMOs) with excellent characteristics such as high yield and good environmental adaptability are entering human life.[1,2] In 2020, the planting area of genetically modified soybean is 96 million hectares, about 78% of the global soybean planting area. However, there are still some controversies in the public about the biosafety of GMOs, demanding the establishment of convenient and sensitive detection methods for GMOs.[3,4]

At present, most detection methods for GMOs are based on polymerase chain reaction (PCR).[5−9] In spite of good detection accuracy and precision, it is difficult for them to carry out extensive field detection because of complicated processes and expensive instruments, which is important for timely and effective market supervision.[10,11] Compared with them, electrochemical biosensors are perhaps a better choice for the development of field detection technology for GMOs.

Electrochemical biosensors are one of the earliest and most mature DNA detection technologies with unique advantages.[12,13] Because signals can be measured directly without requiring an expensive, complicated, and fault-prone transduction device, electrochemical biosensors are of simple operation, high sensitivity, low cost, and easy portability, providing a promising approach for the field detection of GMOs.[14−19] However, sensitivity and specificity need to be further improved because the analyte concentration is usually very low without PCR amplification. Obviously, to construct an electrochemical biosensor for GMOs with high sensitivity and specificity, a novel signal amplification strategy and a new recognition system are greatly demanded. Proven to be a powerful biological cognitive element, the clustered regularly interspaced short palindromic repeats (CRISPR)/Cas system might be an important candidate.[20−22]

The CRISPR/Cas system, that is, CRISPR and CRISPR-associated proteins (Cas), is an RNA-mediated and heritable adaptive immune system that is of widespread existence in bacteria and archaea.[23,24] Under the guidance of CRISPR-derived RNA (crRNA), the Cas protein with endonuclease activity will specifically recognize and cleave the target sequence containing the protospacer adjacent motif (PAM), so the CRISPR/Cas system has excellent selectivity and programmability which can be used to develop biosensors and

Received: September 15, 2021
Accepted: October 15, 2021
Published: October 26, 2021

https://doi.org/10.1021/acs.analchem.1c04022
Anal. Chem. 2021, 93, 14885−14891

Scheme 1. Schematic Diagram of the CRISPR/Cas12a-Mediated Dual-Mode Electrochemical Biosensor for PCR-Free Detection of Genetically Modified Soybean

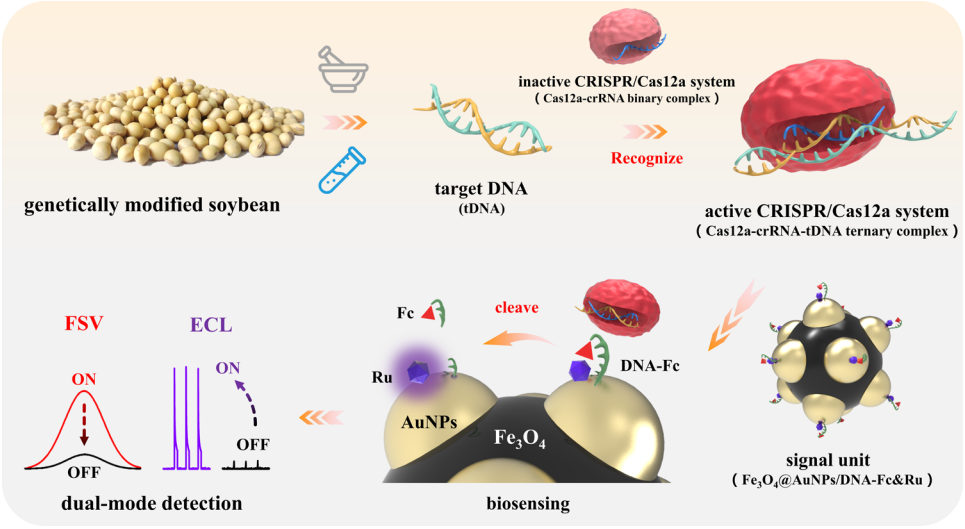

biosensing systems.[25−28] Most studies were based on Cas9, which is the most popular type II enzyme gene-editing tool. It is worth noting that being a member of the Cas protein family, Cas12a can identify the target DNA (tDNA), capture tDNA, and then form a ternary complex with crRNA and tDNA under the guidance of crRNA.[29] In this case, Cas12a is activated to obtain the ability to cleave single-stranded DNA (ssDNA) nonspecifically.[30] Evidently, this signal transduction and amplification process makes it more promising in the development and application of nucleic acid detection than the CRISPR/Cas9 system, the signal amplification capability of which is insufficient because of the lack of nonspecific cleavage ability toward ssDNA.[31−37] As far as we know, there is no report on electrochemical biosensors for the detection of GMOs using the CRISPR/Cas12a system.

In recent years, the dual-mode detection strategy has attracted widespread attention and shown a growing trend in the analysis field, which could cope with the interference from complex sample substrates and improve the detection accuracy.[38−41] For example, tDNA, as a characteristic fragment of a transgene ingredient, exists in a complex sample environment, in which there are a lot of very similar gene sequences and possible impurities with a certain signal response. In this case, a dual-mode detection method can perform cross-validating detection, reduce false negative/positive probability, and thus then obtain more convincing results.

In this study, a dual-mode electrochemical biosensor for the detection of genetically modified soybean SHZD32-1 was developed based on the CRISPR/Cas12a system. The PCR-free detection could be completed in one hour with a limit of detection (LOD) of 0.3 fmol/L. The accuracy and reliability are high because of the fact that electrochemiluminescent (ECL) and fast scan voltammetric (FSV) signals could be cross-validated. This biosensor provides a new solution for the highly sensitive, accurate, and specific field detection of GMOs and new ideas for the application of the CRISPR/Cas12a system in sensor development.

EXPERIMENTAL SECTION

Materials and reagents, apparatus, synthesis of magnetic material Fe_3O_4@AuNPs, and sample processing are displayed in the Supporting Information.

Synthesis of Signal Unit Fe_3O_4@AuNPs/DNA-Fc&Ru. A 200 μL of Fe_3O_4@AuNPs dispersion, 20 μL of 5 mmol/L ruthenium complex (Ru), and 200 μL of 10 μmol/L DNA-Fc which is a short ssDNA modified with ferrocene (Fc) at the 5′ end and sulfhydryl at the 3′ end were mixed. After adjusting the pH to 7.5, incubating at 35 °C for 4 h, adding 200 μL of 2 wt % bovine serum albumin (BSA) to block nonspecific binding sites, removing free DNA-Fc by magnetic washing, and redispersing in 200 μL of water, the signal unit Fe_3O_4@AuNPs/DNA-Fc&Ru dispersion was obtained.

Protocol for the Nonspecific Cleavage of the ssDNA by CRISPR/Cas12a System. A 2 μL of 1 pmol/L Cas12a and 2 μL of 10 pmol/L crRNA were mixed, incubated at room temperature for 10 min, followed by adding 5 μL of tDNA (the sequence of which is identical to the characteristic gene fragment of genetically modified soybean SHZD32-1) standard solution or sample solution containing tDNA, 10 μL of 10× buffer, and 10 μL of the signal unit. After incubating at 37 °C for 45 min, magnetic washing, and separating, the cleaved signal unit could be collected for the subsequent preparation of the electrochemical biosensor.

Preparation of the Electrochemical Biosensor. The uncleaved signal unit or the cleaved signal unit was dropped and firmly adsorbed on the surface of the polished magnetic glassy carbon electrode (MGCE) under the magnetic force. Thus, the electrochemical biosensor could be immediately prepared in only one step, ready for subsequent detection.

ECL Measurement. Using chronoamperometry as excitation, ECL tests were performed in a 0.1 mol/L pH = 7.4 phosphate buffer solution (PBS) containing 20 mmol/L tripropylamine (TPrA). Relevant parameters were set as follows: the potential range was 0−1.5 V, the pulse width was 0.25 s, the pulse period was 30 s, and the voltage of the photomultiplier tube was 800 V.

FSV Measurement. FSV tests were performed in a 0.1 mol/L pH = 7.4 PBS with a potential range −0.5−1.5 V and a scan rate 1000 V/s.

https://doi.org/10.1021/acs.analchem.1c04022
Anal. Chem. 2021, 93, 14885−14891

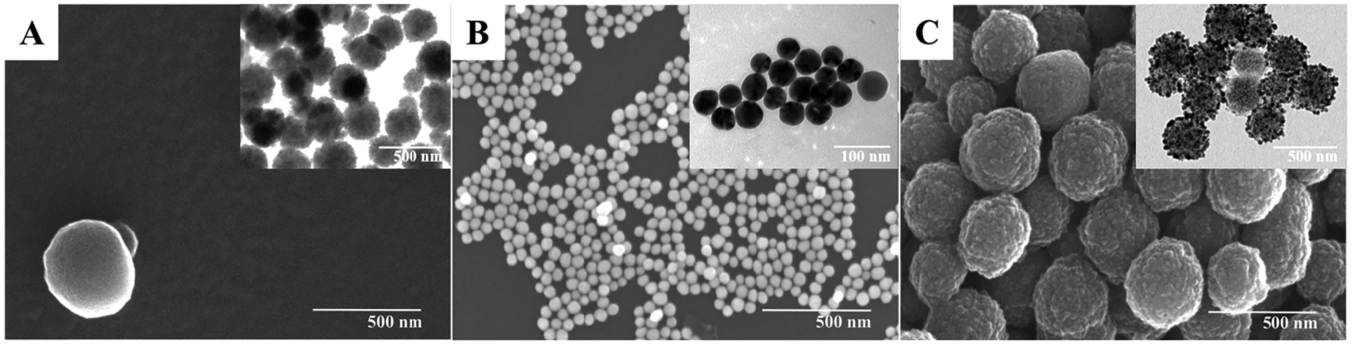

Figure 1. SEM and TEM images of (A) Fe_3O_4NPs, (B) AuNPs, and (C) Fe_3O_4@AuNPs.

RESULTS AND DISCUSSION

Principle of the Dual-Mode Electrochemical Biosensor. The detection mechanism of the CRISPR/Cas12a-mediated dual-mode electrochemical biosensor is shown in Scheme 1. The CRISPR/Cas12a system consists of cas12a and crRNA. Among them, crRNA is composed of repetitive sequences and programmable targeting specific sequences and can be combined with Cas12a to form a Cas12a-crRNA binary complex. Through the specific sequence part of crRNA and the PAM in tDNA, the formed binary complex could specifically recognize and capture tDNA to form a Cas12a-crRNA-tDNA ternary complex. In this case, the nonspecific cleavage ability of the CRISPR/Cas12a system toward ssDNA will be activated. Adopting the abovementioned technical architecture, the electrochemical biosensor is designed based on a functionalized composite bionanomaterial, that is, the signal unit Fe_3O_4@AuNPs/DNA-Fc&Ru. It is Fe_3O_4 nanoparticles (Fe_3O_4NPs) coated with Au nanoparticles (AuNPs), on the surface of which Ru and DNA-Fc are immobilized through Au-N bonds and Au-S bonds, respectively. When the Cas12a-crRNA binary complex, tDNA, and signal unit are present simultaneously, tDNA is recognized and captured by the binary complex through the base complementary pairing between tDNA and crRNA, and the formed ternary complex would activate the nonspecific cleavage ability of Cas12a toward ssDNA. Thus, the single-stranded DNA-Fc immobilized on the signal unit would be cleaved, and the electrochemical label Fc would fall off the surface of the signal unit and enter the solution, resulting in the decrease in the FSV signal from Fc and the synchronous increase in the ECL signal from Ru, which is greatly inhibited by Fc. Both FSV and ECL signals could be used to establish a quantitative relationship with the tDNA concentration, and then determine tDNA in an unknown sample. Employing this sensor construction mode has several advantages for the rapid field detection of tDNA as follows. (1) The signal unit is magnetic and thus convenient for sample pretreatment. In addition, the sensor preparation is so simple as it is to be completed in only one step, bringing good reproducibility. (2) The nonspecific cleavage of ssDNA by the CRISPR/Cas12a system triggered by tDNA has a high-efficiency signal amplification ability without requiring complicated nucleic acid amplification steps. (3) High selectivity could be obtained, benefiting from a dual recognition of the CRISPR/Cas12a system. One is the base complement pairing between crRNA and tDNA, the other is the recognition of PAM in tDNA by the Cas12a protein complex. (4) ECL and FSV signals could mutually verify each other, conducive to avoiding false negative/positive results and then improving the detection accuracy and reliability. Also, (5) the operation process is extremely simple and can be completed in one hour at room temperature, which is suitable for rapid field detection.

Characterization of Nanomaterials. Scanning electron microscopy (SEM) and transmission electron microscopy (TEM) were used to monitor the size and morphology of different nanomaterials. Fe_3O_4NPs (Figure 1A) and AuNPs (Figure 1B) are both uniform nanospheres with a diameter of about 400 and 50 nm, respectively, while magnetic material Fe_3O_4@AuNPs is Fe_3O_4NPs evenly covered by AuNPs (Figure 1C). The energy-dispersive X-ray (EDX) spectrum (Figure S1) shows that the main elements of Fe_3O_4@AuNPs include Fe, O, C, and Au. The abovementioned results indicate that Fe_3O_4@AuNPs were successfully prepared.

Ultraviolet−visible (UV−vis) spectroscopy was used to characterize the synthesis of signal unit Fe_3O_4@AuNPs/DNA-Fc&Ru. As shown in Figure S2, Fe_3O_4NPs have no obvious characteristic absorption peak (curve a), while the characteristic absorption peaks of AuNPs and DNA are located at 526 and 260 nm, respectively (curve b and c). In the case of the signal unit, that of Ru is present at 318 nm in addition to the abovementioned characteristic absorption peaks (curve d), indicating that AuNPs, DNA-Fc, and Ru are all effectively bound onto Fe_3O_4NPs to construct the signal unit.

Characterization of Sensor Assembly. The sensor assembly was characterized by electrochemical impedance spectroscopy (EIS) and cyclic voltammetry (CV) (Supporting Information). As shown in Figure 2A,B, the charge-transfer resistance R_{ct} of bare MGCE is small, and a pair of reversible redox peaks is present (curve a). When Fe_3O_4@AuNPs are assembled onto the electrode surface, R_{ct} decreases a little and peak currents increase a little because of its good electrical conductivity (curve b). In the case of the signal unit (curve c), R_{ct} increases and peak currents decrease significantly because of the negatively charged phosphate backbone of DNA, which hinders the diffusion of the negatively charged redox probe $[Fe(CN)_6]^{3-/4-}$ to the electrode surface and the corresponding charge transfer.[42] As for the cleaved signal unit (curve d), a part of the DNA-Fc sequence in the signal unit is cleaved and falls off the electrode surface, resulting in the reduction of R_{ct} and the increment of peak currents. These results prove that the electrochemical biosensor could be assembled properly.

Feasibility of the Nonspecific Cleavage of ssDNA by the CRISPR/Cas12a System. The feasibility of the nonspecific cleavage of ssDNA by the CRISPR/Cas12a system was demonstrated by polyacrylamide gel electrophoresis (PAGE). As shown in Figure 2C, the band in lane 1 is a 34 nt single-

https://doi.org/10.1021/acs.analchem.1c04022
Anal. Chem. 2021, 93, 14885−14891

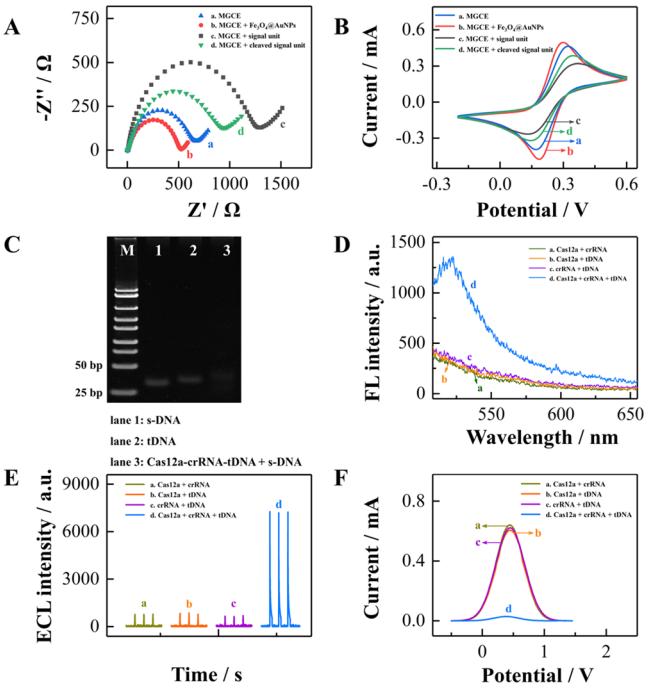

Figure 2. (A) EIS and (B) CV curves of (a) MGCE, (b) MGCE + Fe_3O_4@AuNPs, (c) MGCE + signal unit, and (d) MGCE + cleaved signal unit; (C) PAGE and (D) fluorescence analysis on the feasibility of the nonspecific cleavage of ssDNA by the CRISPR/Cas12a system; (E) ECL and (F) FSV analysis on the feasibility of the dual-mode electrochemical detection.

stranded s-DNA, while the band in lane 2 is the 40 nt tDNA. When the ternary complex Cas12a-crRNA-tDNA and s-DNA were mixed, no obvious band is present in lane 3, demonstrating that s-DNA is cleaved thoroughly. Fluorescence spectroscopy was also used to verify it. A single-stranded 5 nt FQ-DNA modified with the fluorescent reporter group carboxyfluorescein (FAM) at the 5′ end and the fluorescent quenching group black hole quencher (BHQ) at the 3′ end was designed as a nonspecific substrate and fluorescent probe. When the distance between the two groups is small enough, the fluorescence emitted by FAM is quenched by BHQ because of the resonance energy transfer.[43] On the contrary, the fluorescence of FAM could be found with the disappearance of the resonance energy transfer. To test the nonspecific cleavage ability of the CRISPR/Cas12a system toward ssDNA, FQ-DNA was incubated with different mixtures containing Cas12a, crRNA, and tDNA. As shown in Figure 2D, in the absence of tDNA (curve a), crRNA (curve b), or Cas12a (curve c), there is no fluorescence signal of FAM owing to the quenching effect of BHQ. However, in the case that tDNA, crRNA, and Cas12a are all present and form the Cas12a-crRNA-tDNA ternary complex (curve d), the nonspecific cleavage ability of the CRISPR/Cas12a system toward ssDNA is activated, and then, FQ-DNA is effectively cleaved. On this occasion, FAM and BHQ groups are separated, so the fluorescence emission peak of FAM appears at 530 nm. It demonstrates that the CRISPR/Cas12a system has a reliable nonspecific cleavage activity toward ssDNA.

Feasibility of ECL/FSV Dual-Mode Detection. The feasibility of ECL/FSV dual-mode detection was investigated. As shown in Figure 2E,F, when any one of tDNA (curve a), crRNA (curve b), and Cas12a (curve c) is absent, DNA-Fc would not be cleaved without the formation of the Cas12a-crRNA-tDNA ternary complex. Therefore, ECL signals are all weak because of the strong inhibitory effect on the ECL behavior of Ru by Fc through resonance energy transfer.[44−46] However, the FSV signal is strong because DNA-Fc is immobilized on the surface of AuNPs. Fe_3O_4@AuNPs has good electrical conductivity, so it has become a part of the electrode surface because of the equipotential effect. Therefore, DNA-Fc on the surface of AuNPs is as if it is immobilized directly on the electrode surface, and then, electron transfer is very easy, resulting in a strong FSV signal. When the Cas12a-crRNA-tDNA ternary complex is formed (curve d), single-stranded DNA-Fc is cleaved and Fc falls away from the signal unit. In this case, the distance between Fc and Ru, which is still on the surface of the signal unit, increases sharply, and the inhibitory effect on the ECL of Ru is lost, resulting in a significant increment in the ECL intensity. At the same time, the increment in the distance between Fc and the electrode surface also leads to a weakened FSV signal. ECL and FSV signal changes are generated by the same cleavage action, meaning that dual-mode detection could be obtained conveniently.

Optimization of Experimental Conditions. The optimal experimental conditions were obtained using 10^7 fmol/L tDNA standard solution as the test one. From Figure S3, it can be concluded that the optimal experimental conditions are as follows: incubation time, that is, nonspecific cleaving time is 45 min; incubation temperature is 37 °C; buffer pH in ECL detection is 8.0; and TPrA concentration is 30 mmol/L. Also, the optimal amount ratio of Ru to DNA-Fc is 50:1 in the synthesis of signal units (Figure S4).

Linear Relationship and Sensitivity. Under the optimal experimental conditions, the analytical performance of this dual-mode electrochemical biosensor was studied by detecting a series of tDNA standard solutions at different concentrations of 1, 10, 10^2, 10^3, 10^4, 10^5, 10^6, 10^7, and 10^8 fmol/L. As shown in Figure 3A, the ECL intensity increases with the increment in the tDNA concentration. There is a good linear relationship between the ECL intensity and the logarithm of the tDNA

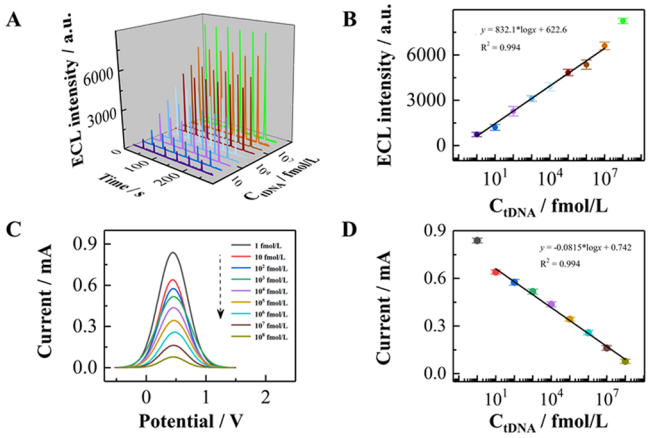

Figure 3. (A) ECL response curves of the electrochemical biosensor at different tDNA concentrations from 1 to 10^8 fmol/L; (B) linear relationship of ECL intensity versus logarithm of tDNA concentration; (C) current response curves of the electrochemical biosensor at different tDNA concentrations from 1 to 10^8 fmol/L; and (D) linear relationship of peak current versus logarithm of tDNA concentration.

https://doi.org/10.1021/acs.analchem.1c04022
Anal. Chem. 2021, 93, 14885−14891

Table 1. Recovery Tests for SHZD32-1 in Spiked Soybean Samples ($\bar{x} \pm s$, $n = 5$)

		ECL			FSV		
sample no.	added (fmol/L)	found (fmol/L)	recovery (%)	RSD (%)	found (fmol/L)	recovery (%)	RSD (%)
1	1.000×10^2	$(1.087 \pm 0.092) \times 10^2$	108.7	8.5	$(0.948 \pm 0.069) \times 10^2$	94.8	7.3
2	1.000×10^3	$(0.954 \pm 0.063) \times 10^3$	95.4	6.6	$(1.137 \pm 0.105) \times 10^3$	113.7	9.2
3	1.000×10^4	$(0.977 \pm 0.038) \times 10^4$	97.7	3.9	$(0.965 \pm 0.102) \times 10^4$	96.5	10.6
4	1.000×10^5	$(1.121 \pm 0.054) \times 10^5$	112.1	4.8	$(0.893 \pm 0.037) \times 10^5$	89.3	4.1
5	1.000×10^6	$(0.903 \pm 0.086) \times 10^6$	90.3	9.5	$(1.036 \pm 0.042) \times 10^6$	103.6	4.1
6	1.000×10^7	$(1.078 \pm 0.055) \times 10^7$	107.8	5.1	$(1.034 \pm 0.075) \times 10^7$	103.4	7.3

concentration in the range of $1-10^7$ fmol/L (Figure 3B). The linear regression equation is $y = 832.1*\log x + 622.6$ with a squared correlation coefficient $R^2 = 0.994$, where y is the ECL intensity (a.u.) and x is the tDNA concentration (fmol/L). The LOD could be roughly estimated as 0.3 fmol/L. In the case of FSV, the peak current gradually decreases as the tDNA concentration increases (Figure 3C), and the peak current shows a good linear relationship with the logarithm of the tDNA concentration in the range of $10-10^8$ fmol/L (Figure 3D). The corresponding linear regression equation is $y = -0.0815*\log x + 0.742$ with $R^2 = 0.994$, where y is the peak current (mA) and x is the tDNA concentration (fmol/L). The LOD was about 3 fmol/L. Compared with the previously reported electrochemical biosensors for the detection of GMOs (Table S2), the detection sensitivity of this one is higher because of the following reasons: (1) after combining with tDNA to form a ternary complex, the nonspecific cleavage ability of the CRISPR/Cas12a system toward ssDNA is activated, and therefore, the single-stranded DNA-Fc immobilized on the signal unit is cleaved continuously by the ternary complex, achieving effective signal amplification; (2) using electrons as excitation, the ECL method has inherently high sensitivity without the interference of background lights; and (3) the Faradaic peak current of FSV linearly increases with the scan rate (Figure S5).[47,48] Although the charging current also increases linearly with the scan rate, it is a constant value and can be easily deducted. Therefore, detection sensitivity could be significantly increased.

Accuracy and Precision. To evaluate the accuracy and precision, a series of standard addition solutions at different concentrations prepared by spiking tDNA into the extraction solution of the SHZD32-1 negative soybean sample were tested. As shown in Table 1, recoveries of ECL detection are 90.3−112.1% with relative standard deviations (RSDs) of 3.9−9.5%, while recoveries of FSV detection are 89.3−113.7% with RSDs 4.1−10.6%, indicating that this dual-mode electrochemical biosensor has satisfactory accuracy and precision.

Stability and Selectivity. Signal stability is also an important indicator of electrochemical biosensors. The stability of the ECL signal was checked by 20 cycles of continuous potential scan, using 10^5 fmol/L tDNA standard solution. It could be found that the ECL intensity did not change significantly, with an RSD of 2.0%. In the case of FSV, the RSD is 2.3% (Figure 4A). Therefore, the signal stability of the electrochemical biosensor is good. The stability of the signal unit was also evaluated by testing 10^5 fmol/L tDNA for 10 consecutive days, which was stored at 4 °C. As shown in Figure 4B, satisfactory stability could be obtained, benefiting from the especially simple bionanomaterial preparation and biosensor construction.

The selectivity of the electrochemical biosensor was evaluated by seven control experiments, including the blank,

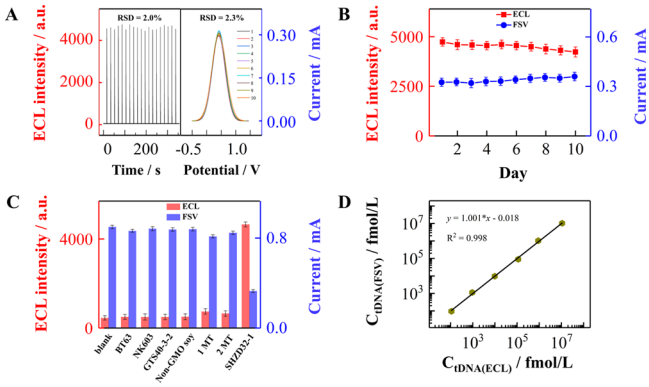

Figure 4. (A) ECL and FSV signal stability of the electrochemical biosensor. (B) Stability of the signal unit. (C) ECL and FSV selectivity of the electrochemical biosensor. The concentration of tDNA is 10^5 fmol/L. (D) Correlation of the detection results between ECL and FSV methods.

genetically modified corn BT63, genetically modified corn NK603, genetically modified soybean GTS40-3-2, non-GMO soy, single-base mismatched target (1 MT), and two-base mismatched target (2 MT). Results (Figure 4C) show that the signal intensities of the four crops and the two mismatched targets used as the control are close to that of the blank, while a much stronger ECL signal and a much lower FSV signal are obtained in the case of genetically modified soybean SHZD32-1, demonstrating an excellent selectivity of the dual-mode electrochemical biosensor.

Consistency of ECL and FSV Results. The consistency between ECL and FSV results was studied using the data in Table 1, and the results are shown in Figure 4D. The linear regression equation is $y = 1.001*x - 0.018$, where y is the tDNA concentration found by FSV, and x is the tDNA concentration found by ECL. The slope is 1.001, the intercept is −0.018, and R^2 is 0.998, indicating that the test results of the two methods are highly consistent and can be cross-validated. It helps avoid false negative/positive results that may be likely in a single-mode method.

Analysis of Real SHZD32-1 Samples. To verify whether the proposed dual-mode electrochemical biosensor can detect real samples sensitively and specifically, quantitative detection of genetically modified soybean SHZD32-1 samples was carried out using this biosensor and national standard PCR method,[49] the results of which are shown in Table 2. The intergroup t test was used to check the significant difference between the two groups. It could be found that the t value between ECL and qRT-PCR is 1.12 and that between FSV and qRT-PCR is 1.05. They are both much smaller than $t_{0.05,4} = 2.78$, showing very good reliability and practicality.

https://doi.org/10.1021/acs.analchem.1c04022
Anal. Chem. 2021, 93, 14885−14891

Table 2. Detection of Real SHZD32-1 Soybean Samples

sample	qRT-PCR (fmol/L)	ECL (fmol/L)	FSV (fmol/L)
SHZD32-1	6.59×10^5	6.25×10^5	6.41×10^5
	6.67×10^5	6.39×10^5	6.58×10^5
	6.43×10^5	6.58×10^5	6.69×10^5
	6.48×10^5	6.61×10^5	6.47×10^5
	6.55×10^5	6.43×10^5	6.24×10^5

To realize the rapid field detection of GMOs, a portable equipment with both ECL and FSV testing capabilities is still required, which is being developed in our group.[50,51]

CONCLUSIONS

In summary, a dual-mode electrochemical biosensor for the detection of genetically modified soybean was developed based on the CRISPR/Cas12a system, which has significant advantages in the following aspects: (1) High sensitivity—the LOD was as low as 0.3 fmol/L, affording the detection of low-concentration genetically modified ingredients. (2) High selectivity—common interferences will not affect the detection. (3) High accuracy and precision—satisfactory recoveries and RSDs could be obtained, which are no more than 114 and 11%, respectively. (4) High reliability—ECL and FSV signals can be cross-validated, which helps avoid false negative/positive results. (5) Simple steps—Once the signal unit is prepared, the detection could be accomplished in just one step. (6) Mild experimental conditions—it could be carried out at ambient temperature without PCR amplification. Lastly, (7) high speed—it could be completed in one hour. Therefore, this dual-mode electrochemical biosensor has good application potential in the field of rapid detection of genetically modified crops and products.

ASSOCIATED CONTENT

Supporting Information

The Supporting Information is available free of charge at https://pubs.acs.org/doi/10.1021/acs.analchem.1c04022.

All DNA and RNA sequences in the present work; comparison of the linear range and sensitivity of previously reported electrochemical DNA biosensors for GM crops; EDX of Fe_3O_4@AuNPs; UV-vis spectroscopy of (a) Fe_3O_4NPs, (b) Fe_3O_4@AuNPs, (c) Fe_3O_4@AuNPs/DNA-Fc, and (d) signal unit; optimization of (A) incubation temperature, (B) incubation time, (C) pH of PBS in ECL, and (D) coreaction reagent TPrA concentration in ECL; relationship between the ECL intensity and $C_{Ru}/C_{DNA\text{-}Fc}$ concentration ratio; and FSV curves of 10^5 fmol/L tDNA at different scan rates (200, 300, 400, 500, 600, 700, 800, 900, and 1000 V/s) and (B) linear relationship of current versus scan rates (PDF)

AUTHOR INFORMATION

Corresponding Authors

Xiaofu Wang − *State Key Laboratory for Managing Biotic and Chemical Threats to the Quality and Safety of Agro-products, Zhejiang Academy of Agricultural Sciences, Hangzhou 310021, P.R. China*; orcid.org/0000-0001-9323-4022; Email: yywxf1981@163.com

Zhiyong Guo − *State Key Laboratory for Managing Biotic and Chemical Threats to the Quality and Safety of Agro-products, School of Material Science and Chemical Engineering, Ningbo University, Ningbo 315211, P.R. China*; orcid.org/0000-0003-1288-1573; Email: guozhiyong@nbu.edu.cn

Authors

Haoran Ge − *State Key Laboratory for Managing Biotic and Chemical Threats to the Quality and Safety of Agro-products, School of Material Science and Chemical Engineering, Ningbo University, Ningbo 315211, P.R. China*

Junfeng Xu − *State Key Laboratory for Managing Biotic and Chemical Threats to the Quality and Safety of Agro-products, Zhejiang Academy of Agricultural Sciences, Hangzhou 310021, P.R. China*

Han Lin − *State Key Laboratory for Managing Biotic and Chemical Threats to the Quality and Safety of Agro-products, School of Material Science and Chemical Engineering, Ningbo University, Ningbo 315211, P.R. China*

Huiqian Zhou − *State Key Laboratory for Managing Biotic and Chemical Threats to the Quality and Safety of Agro-products, School of Material Science and Chemical Engineering, Ningbo University, Ningbo 315211, P.R. China*

Tingting Hao − *State Key Laboratory for Managing Biotic and Chemical Threats to the Quality and Safety of Agro-products, School of Material Science and Chemical Engineering, Ningbo University, Ningbo 315211, P.R. China*

Yangbo Wu − *Faculty of Electrical Engineering and Computer Science, Ningbo University, Ningbo 315211, P.R. China*

Complete contact information is available at: https://pubs.acs.org/10.1021/acs.analchem.1c04022

Author Contributions

The manuscript was written through contributions of all authors. All authors have approved the final version of the manuscript.

Notes

The authors declare no competing financial interest.

ACKNOWLEDGMENTS

We gratefully acknowledge the National Natural Science Foundation of China (Grant No. 42076193, 81773483, and 31772098), Ningbo Science and Technology Bureau (202002 N3061), and State Key Laboratory for Managing Biotic and Chemical Threats to the Quality and Safety of Agro-products (ZS20190101). This work was also sponsored by K.C. Wong Magna Fund at Ningbo University.

REFERENCES

(1) Mills, G.; Sharps, K.; Simpson, D.; Pleijel, H.; Frei, M.; Burkey, K.; Emberson, L.; Uddling, J.; Broberg, M.; Feng, Z.; Kobayashi, K.; Agrawal, M. *Glob. Chang. Biol.* **2018**, *24*, 4869−4893.

(2) Nelson, R.; Wiesner-Hanks, T.; Wisser, R.; Balint-Kurti, P. *Nat. Rev. Genet.* **2018**, *19*, 21−33.

(3) Tabashnik, B. E.; Brevault, T.; Carriere, Y. *Nat. Biotechnol.* **2013**, *31*, 510−521.

(4) Fraiture, M. A.; Herman, P.; De Loose, M.; Debode, F.; Roosens, N. H. *Trends Biotechnol.* **2017**, *35*, 508−517.

(5) Xiao, B.; Niu, C.; Shang, Y.; Xu, Y.; Huang, K.; Zhang, X.; Xu, W. *Food Chem.* **2020**, *330*, No. 127247.

(6) Jacobs, B. K. M.; Goetghebeur, E.; Vandesompele, J.; De Ganck, A.; Nijs, N.; Beckers, A.; Papazova, N.; Roosens, N. H.; Clement, L. *Anal. Chem.* **2017**, *89*, 4461−4467.

(7) Bogozalec Kosir, A.; Demsar, T.; Stebih, D.; Zel, J.; Milavec, M. *Food Chem.* **2019**, *294*, 73−78.

(8) Fraiture, M. A.; Herman, P.; Papazova, N.; De Loose, M.; Deforce, D.; Ruttink, T.; Roosens, N. H. *Food Chem.* **2017**, *232*, 351−358.
(9) Glowacka, K.; Kromdijk, J.; Leonelli, L.; Niyogi, K. K.; Clemente, T. E.; Long, S. P. *Plant Cell Environ.* **2016**, *39*, 908−917.
(10) Li, Y.; Sun, L.; Qian, J.; Wang, C.; Liu, Q.; Han, E.; Hao, N.; Zhang, L.; Cai, J.; Wang, K. *Anal. Chim. Acta* **2016**, *948*, 90−97.
(11) Rosa, S. F.; Gatto, F.; Angers-Loustau, A.; Petrillo, M.; Kreysa, J.; Querci, M. *Food Chem.* **2016**, *201*, 110−119.
(12) Ang, W. L.; Seah, X. Y.; Koh, P. C.; Caroline, C.; Bonanni, A. *ACS Appl. Nano Mater.* **2020**, *3*, 5489−5498.
(13) Placido, A.; Pereira, C.; Guedes, A.; Barroso, M. F.; Miranda-Castro, R.; de Los-Santos-Alvarez, N.; Delerue-Matos, C. *Biosens. Bioelectron.* **2018**, *110*, 147−154.
(14) Fortunati, S.; Rozzi, A.; Curti, F.; Giannetto, M.; Corradini, R.; Careri, M. *Biosens. Bioelectron.* **2019**, *129*, 7−14.
(15) Wang, D.; Xiao, X.; Xu, S.; Liu, Y.; Li, Y. *Biosens. Bioelectron.* **2018**, *99*, 431−437.
(16) Liu, F.; Li, K.; Zhang, Y.; Ding, J.; Wen, T.; Pei, X.; Yan, Y.; Ji, W.; Liu, J.; Zhang, X.; Li, L. *Microchim. Acta* **2020**, *187*, 574.
(17) Gao, H.; Wen, L.; Tian, J.; Wu, Y.; Liu, F.; Lin, Y.; Hua, W.; Wu, G. *Biosens. Bioelectron.* **2019**, *142*, No. 111504.
(18) Li, Y.; Sun, L.; Liu, Q.; Han, E.; Hao, N.; Zhang, L.; Wang, S.; Cai, J.; Wang, K. *Talanta* **2016**, *161*, 211−218.
(19) Ye, Y.; Mao, S.; He, S.; Xu, X.; Cao, X.; Wei, Z.; Gunasekaran, S. *Talanta* **2020**, *206*, No. 120205.
(20) Gootenberg, J. S.; Abudayyeh, O. O.; Lee, J. W.; Essletzbichler, P.; Dy, A. J.; Joung, J.; Daringer, N. M.; Frejie, C. A.; Myhrvold, C.; Bhattacharyya, R. P.; Livuy, J.; Regev, A.; Koonin, E. V.; Hung, D. T.; Sabeti, P. C.; Collins, J. J.; Zhang, F. *Science* **2017**, *356*, 483−442.
(21) Jiao, C.; Sharma, S.; Dugar, G.; Peeck, N. L.; Bischler, T.; Wimmer, F.; Yu, Y.; Barquist, L.; Schoen, C.; Kurzai, O.; Sharma, C. M.; Beusel, C. L. *Science* **2021**, *372*, 941−948.
(22) Liang, M.; Li, Z.; Wang, W.; Liu, J.; Liu, L.; Zhu, G.; Karthik, L.; Wang, M.; Wang, K.; Wang, Z.; Yu, J.; Shuai, Y.; Yu, J.; Zhang, L.; Yang, Z.; Li, C.; Zhang, Q.; Shi, T.; Zhou, L.; Xie, F.; Dai, H.; Liu, X.; Zhang, J.; Liu, G.; Zhou, Y.; Zhang, B.; Liu, C.; Li, S.; Xia, X.; Tong, Y.; Liu, Y.; Alterovitz, G.; Tan, G.; Zhang, L. *Nat. Commun.* **2019**, *10*, 3672.
(23) Murugan, K.; Babu, K.; Sundaresan, R.; Rajan, R.; Sashital, D. G. *Mol. Cell* **2017**, *68*, 15−25.
(24) Jackson, S. A.; McKenzie, R. E.; Fagerlund, R. D.; Kieper, S. N.; Fineran, P. C.; Brouns, S. J. *Science* **2017**, *356*, No. eaal5056.
(25) Li, Y.; Li, S.; Wang, J.; Liu, G. *Trends Biotechnol.* **2019**, *37*, 730−743.
(26) Sun, X.; Wang, Y.; Zhang, L.; Liu, S.; Zhang, M.; Wang, J.; Ning, B.; Peng, Y.; He, J.; Hu, Y.; Gao, Z. *Anal. Chem.* **2020**, *92*, 3032−3041.
(27) Wang, X.; Xiong, E.; Tian, T.; Cheng, M.; Lin, W.; Wang, H.; Zhang, G.; Sun, J.; Zhou, X. *ACS Nano* **2020**, *14*, 2497−2508.
(28) Uygun, Z. O.; Yeniay, L.; Gi Rgi, N. S. F. *Anal. Chim. Acta* **2020**, *1121*, 35−41.
(29) Pickar-Oliver, A.; Gersbach, C. A. *Nat. Rev. Mol. Cell Biol.* **2019**, *20*, 490−507.
(30) Chen, J. S.; Ma, E.; Harrington, L. B.; Costa, M. D.; Tian, X.; Palefsky, J. M.; Doudna, J. A. *Science* **2018**, *360*, 436−439.
(31) Li, F.; Ye, Q.; Chen, M.; Zhou, B.; Zhang, J.; Pang, R.; Xue, L.; Wang, J.; Zeng, H.; Wu, S.; Zhang, Y.; Ding, Y.; Wu, Q. *Biosens. Bioelectron.* **2021**, *179*, No. 113073.
(32) Dai, Y.; Somoza, R. A.; Wang, L.; Welter, J. F.; Li, Y.; Caplan, A. I.; Liu, C. C. *Angew. Chem. Int. Ed.* **2019**, *58*, 17399−17405.
(33) Huang, C. H.; Lee, K. C.; Doudna, J. A. *Trends Cancer* **2018**, *4*, 499−512.
(34) Lee, Y.; Choi, J.; Han, H.-K.; Park, S.; Park, S. Y.; Park, C.; Baek, C.; Lee, T.; Min, J. *Sensor. Actuat. B-Chem.* **2021**, *326*, No. 128677.
(35) Liu, H.; Wang, J.; Zeng, H.; Liu, X.; Jiang, W.; Wang, Y.; Ouyang, W.; Tang, X. *Food Chem.* **2021**, *334*, No. 127608.
(36) Wu, H.; Qian, C.; Wu, C.; Wang, Z.; Wang, D.; Ye, Z.; Ping, J.; Wu, J.; Ji, F. *Biosens. Bioelectron.* **2020**, *157*, No. 112153.
(37) Zhang, D.; Yan, Y.; Que, H.; Yang, T.; Cheng, X.; Ding, S.; Zhang, X.; Cheng, W. *ACS Sens.* **2020**, *5*, 557−562.
(38) Zhou, H.; Zhang, J.; Li, B.; Liu, J.; Xu, J. J.; Chen, H. H. *Anal. Chem.* **2021**, *93*, 6120−6127.
(39) Yang, H.; Wang, C.; Xu, E.; Wei, W.; Liu, Y.; Liu, S. *Anal. Chem.* **2021**, *93*, 6567−6572.
(40) Chen, B.; Xiao, G.; He, M.; Hu, B. *Anal. Chem.* **2021**, *93*, 9454−9461.
(41) Zhou, J.; Ren, M.; Wang, W.; Huang, L.; Lu, Z.; Song, Z.; Foda, M. F.; Zhao, L.; Han, H. *Anal. Chem.* **2020**, *92*, 8802−8809.
(42) Dai, Y.; Chiu, L. Y.; Chen, Y.; Qin, S.; Wu, X.; Liu, C. C. *ACS Sens.* **2019**, *4*, 161−169.
(43) Gao, X.; Li, H.; Zhao, Y.; Jie, G. *Biosens. Bioelectron.* **2019**, *143*, No. 111602.
(44) Peng, L.; Yuan, Y.; Fu, X.; Fu, A.; Zhang, P.; Chai, Y.; Gan, X.; Yuan, R. *Anal. Chem.* **2019**, *91*, 3239−3245.
(45) Wang, H.; Song, Y.; Chai, Y.; Yuan, R. *Biosens. Bioelectron.* **2019**, *140*, No. 111344.
(46) Zhu, L.; Zhang, M.; Ye, J.; Yan, M.; Zhu, Q.; Huang, J.; Yang, X. *Anal. Chem.* **2020**, *92*, 8614−8622.
(47) Amatore, C.; Bouret, Y.; Maisonhaute, E.; Abruña, H. D.; Goldsmith, J. I. *C. R. Chim.* **2003**, *6*, 99−115.
(48) Zhou, H.; Han, T.; Wei, Q.; Zhang, S. *Anal. Chem.* **2016**, *88*, 2976−2983.
(49) Event-specific Method for the Detection of Genetically Modified Plants. *The Standardization Administration of the People's Republic of China*, SN/T 2668−2010.
(50) Xiao, F.; Zhou, H.; Lin, H.; Li, H.; Zou, T.; Wu, Y.; Guo, Z. *Anal. Chim. Acta* **2021**, *1175*, No. 338744.
(51) Chen, G.; Xie, J.; Zhang, Z.; Meng, W.; Zhang, C.; Kang, K.; Wu, Y.; Guo, Z. *Sensor. Actuat. B-Chem.* **2019**, *307*, 127135.

https://doi.org/10.1021/acs.analchem.1c04022
Anal. Chem. 2021, 93, 14885−14891